Inverse Problems 6 (1990) 133–151. Printed in the UK

Inversion of the Bloch transform in magnetic resonance imaging using asymmetric two-component inverse scattering

Andrew E Yagle
Department of Electrical Engineering and Computer Science, The University of Michigan, Ann Arbor, MI 48109-2122, USA

Received 28 April 1989, in final form 15 August 1989

Abstract. In magnetic resonance imaging, the relation between the radio-frequency modulation of the magnetic field and the desired final magnetisation state is called the Bloch transform. Selective excitation then amounts to inverting this transform, which is highly nonlinear. Previous attempts to formulate this problem as an inverse scattering problem have restricted attention to solutions using reflectionless potentials. This paper uses fast numerical algorithms for inverse scattering problems to obtain a much larger set of solutions. Numerical examples are included.

1. Introduction

In magnetic resonance imaging (MRI), a magnetic field is applied to align proton spins. Another magnetic field, transverse to the first field, is then modulated using radio-frequency (RF) modulation in such a way that the axes of the proton spins in a selected region are rotated or flipped, relative to those in the rest of the object being imaged. The superposition of the proton spins results in a net magnetisation. When the modulation stops, the proton spin axes return to the original aligned direction, radiating at the Larmor frequency; the time constant of this relaxation gives information about the composition of the object in the selected region. For more details on MRI see [1].

To achieve selective excitation (of proton spins) in the object being imaged, the transverse magnetic field must be modulated in such a way that only the proton spins in a thin slice of the object are flipped; the spins in the rest of the object must be unaltered when the modulation stops. Then the radiation and relaxation time information are known to apply solely to the selected thin slice. Typically, the spins are to be flipped 90° or 180° in a thin slice, and not flipped elsewhere; in any case the desired final magnetisation state is known.

The relation between the RF modulation pulse and the magnetisation state resulting from it is a complicated relation called the Bloch transform [2]. The problem of determining what RF modulation to use to achieve a desired magnetisation is thus the inversion of the Bloch transform.

Several approaches have been used here. The most straightforward is to linearise the Bloch transform into a Fourier transform [3]. This is the so-called 'small tip angle' approximation. An interesting interpretation of this approximation, in the context of the scattering formulation used in this paper, is given in section 4.4 below. Other approaches have been taken in [4–6]; the optimal control problem formulation in [6] is notable.

0266-5611/90/010133+19$03.50

The most promising approach has been the inverse scattering formulation due to Grunbaum and his co-workers, notably Hasenfeld. The inverse Bloch transform can be transformed into a Schrödinger equation inverse potential problem by stereographically projecting the magnetisation [7–10]. The inverse scattering transform maps solutions of the Schrödinger equation associated with reflectionless potentials to solutions of the Korteweg–de Vries equation [11]. This allows the body of knowledge on the latter equation to be applied to this problem.

A recent paper by Grunbaum [12] transforms the inverse Bloch transform into a two-component wave system inverse scattering problem of Zakharov–Shabat type (see [11]). This is much more promising, since fast algorithms for solving inverse scattering problems for asymmetric two-component systems [13] can now be directly applied to this problem.

This paper applies the fast algorithms of [13] to the two-component wave system inverse scattering formulation of the inverse Bloch transform. The result is a numerical procedure for computing the RF magnetic field modulation needed to achieve a desired final magnetisation state. By considering non-reflectionless potentials, a much greater range of solutions is made available.

The paper is organised as follows. In section 2 we review the Bloch transform, and the reformulation of the inverse Bloch transform as a two-component wave system inverse scattering problem [12]. In section 3 we review the pertinent results of [13] on solving this inverse scattering problem. In section 4 we apply the results of section 3 to the problem posed in section 2. Section 5 presents some numerical examples of the new procedure. Section 6 concludes by summarising the results and noting directions for future research.

2. The Bloch transform and inverse scattering

2.1. The Bloch transform

Let $M(x,y,z,t)$ be the magnetisation due to proton spins aligning locally with an imposed magnetic field $B(x,y,z,t)$. Since the RF magnetic field modulation is short in duration (about 3 ms), the decay terms in the Bloch equations can be neglected, resulting in

$$\frac{\mathrm{d}}{\mathrm{d}t}M(x,y,z,t) = \gamma B(x,y,z,t) \times M(x,y,z,t) \tag{2.1}$$

where γ is the gyromagnetic ratio of the atomic nucleus. γ varies with the size of the nucleus; for protons γ=4260 Hz G^{-1}.

The magnetic field has three components: a strong (about 10 000 G = 1 T) constant component B_o in the z direction; a component Gz in the z direction varying linearly with z (about 1 G cm^{-1}); and a time-varying RF-modulated component in the x,y plane. Thus

$$B(x,y,z,t) = B_1(t)(\cos\omega_1(t)\boldsymbol{i} + \sin\omega_1(t)\boldsymbol{j}) + (B_o + Gz)\boldsymbol{k}. \tag{2.2}$$

Here $B_1(t)$ is the amplitude modulation and

$$\phi(t) = \omega_1(t) - \omega_L t \qquad \omega_L = \gamma B_o \tag{2.3}$$

is the phase modulation of the transverse magnetic field in the x, y plane. Note that ω_L is the Larmor frequency of precession of the proton spins at $z = 0$.

Following [1] we transform to coordinates rotating at ω_L:

$$N(x,y,z,t) = \begin{pmatrix} \cos\omega_L t & -\sin\omega_L t & 0 \\ \sin\omega_L t & \cos\omega_L t & 0 \\ 0 & 0 & 1 \end{pmatrix} M(x,y,z,t). \tag{2.4}$$

Using (2.2)–(2.4), the Bloch equations (2.1) become

$$\frac{dN}{dt} = \begin{pmatrix} 0 & \Delta\omega & -\gamma B_1 \sin\phi \\ -\Delta\omega & 0 & \gamma B_1 \cos\phi \\ \gamma B_1 \sin\phi & -\gamma B_1 \cos\phi & 0 \end{pmatrix} N(x,y,\Delta\omega,t) \tag{2.5}$$

where spatial position along the z axis has been replaced by

$$\Delta\omega = \gamma G z. \tag{2.6}$$

In (2.5), $\Delta\omega = \gamma G z$ is the difference between the local Larmor frequency at z and the Larmor frequency ω_L at $z = 0$. Note that the gradient in the magnetic field along the z axis has produced spatial encoding; position along the z axis has been replaced by the offset $\Delta\omega$ in resonant frequency from ω_L. Since $B_o \approx 10000$ G and $G \approx 1$ G cm^{-1}, $\Delta\omega$ is an offset in kHz from an ω_L in the MHz range.

Equation (2.5) describes how the rotating magnetisation vector $N(x,y,z,t)$ evolves in time for a given modulation $\{B_1(t), \phi(t)\}$. The final magnetisation state $N(x,y,z,T)$ is found by integrating (2.5) from $t = 0$ to $t = T$, where T is the length of the RF modulation pulse. Hence (2.5) implements the Bloch transform [2]

$$\mathscr{B}\{B_1(t), \phi(t), 0 \le t \le T\} \to N(x,y,z,T). \tag{2.7}$$

In the following, we confine our attention to the initial magnetisation state

$$M(x,y,z,0) = N(x,y,z,0) = [0,0,-1]^T \tag{2.8}$$

(i.e. all proton spins are aligned in the $-z$ direction), and to final magnetisation states with no x and y variation. This means that all x and y dependencies can be dropped in the following, leaving dependencies on offset frequency $\Delta\omega$ (in lieu of z) and time t.

2.2. Transformation to a two-component wave system

Here we follow [12] and transform (2.5) to a two-component wave system of Zakharov–Shabat type. This is a special case of the asymmetric two-component system treated in [13].

Consider the density matrix $P(t,\Delta\omega)$ defined from $N(t,\Delta\omega) = [N_x, N_y, N_z]^T$ by

$$\begin{aligned} P(t,\Delta\omega) &= \frac{i}{2}\begin{pmatrix} -N_z & N_x - iN_y \\ N_x + iN_y & N_z \end{pmatrix} \\ &= \frac{i}{2}\begin{pmatrix} 0 & 1 \\ 1 & 0 \end{pmatrix} N_x + \frac{i}{2}\begin{pmatrix} 0 & -i \\ i & 0 \end{pmatrix} N_y + \frac{i}{2}\begin{pmatrix} -1 & 0 \\ 0 & 1 \end{pmatrix} N_z. \end{aligned} \tag{2.9}$$

The set of matrices are the Pauli spin matrices; they show why we choose this particular $P(t,\Delta\omega)$.

Since the system matrix in (2.5) is antisymmetric, $||N(t,\Delta\omega)||$ does not vary with time t. Hence the eigenvalues $\pm(\mathrm{i}/2)\sqrt{||N(t,\Delta\omega)||}$ of $P(t,\Delta\omega)$ are also independent of t. This implies that the time evolution of $P(t,\Delta\omega)$ can be described by a unitary transformation

$$P(t,\Delta\omega) = U(t,\Delta\omega)P(0,\Delta\omega)U^{\mathrm{H}}(t,\Delta\omega) \tag{2.10a}$$

$$U(t,\Delta\omega) = \begin{pmatrix} \alpha(t,\Delta\omega) & \beta(t,\Delta\omega) \\ -\beta^*(t,\Delta\omega) & \alpha^*(t,\Delta\omega) \end{pmatrix} \tag{2.10b}$$

$$|\alpha(t,\Delta\omega)|^2 + |\beta(t,\Delta\omega)|^2 = 1. \tag{2.10c}$$

At this point our derivation diverges from that of [12]. Define the matrix $D = (\mathrm{d}U/\mathrm{d}t)U^{-1}$, so that

$$\frac{\mathrm{d}U}{\mathrm{d}t}(t,\Delta\omega) = DU(t,\Delta\omega) = \begin{pmatrix} d(t,\Delta\omega) & e(t,\Delta\omega) \\ -e^*(t,\Delta\omega) & d^*(t,\Delta\omega) \end{pmatrix} U(t,\Delta\omega). \tag{2.11}$$

The symmetries in D can be seen by exchanging rows and columns in (2.11) and using (2.10*b*). Differentiating (2.10*a*) with respect to t, inserting (2.11) and then (2.9), and finally comparing with (2.5) yields

$$\frac{\mathrm{d}}{\mathrm{d}t}\begin{pmatrix} \beta(t,\Delta\omega) \\ \alpha^*(t,\Delta\omega) \end{pmatrix} = \begin{pmatrix} \mathrm{i}\Delta\omega/2 & r(t) \\ -r^*(t) & -\mathrm{i}\Delta\omega/2 \end{pmatrix}\begin{pmatrix} \beta(t,\Delta\omega) \\ \alpha^*(t,\Delta\omega) \end{pmatrix} \tag{2.12a}$$

$$r(t) = (\mathrm{i}/2)\gamma B_1(t)\mathrm{e}^{\mathrm{i}\phi(t)}. \tag{2.12b}$$

Equations (2.12), which appeared in [12], are an asymmetric two-component wave system of Zakharov–Shabat type [11]. They are a special case of the asymmetric two-component wave system considered in [13] (specifically, $s(z) = -r^*(z)$ in (2.1) of [13]). Note that in (2.12) time t takes the role of spatial position, and resonance offset $\Delta\omega$ takes the role of wavenumber.

2.3. Comments

It is not surprising that an asymmetric two-component wave system arises here. The Schrödinger equation formulation of the Bloch transform used in [7–10] has a complex potential with its imaginary part proportional to energy, when phase modulation is allowed [12]. Such potentials are associated with absorbing media [14], and absorbing media are known to be readily handled using asymmetric two-component wave systems [13].

An alternative to (2.12) is the Riccati equation associated with this scattering system. Define

$$R(t,\Delta\omega) = \frac{\beta(t,\Delta\omega)}{\alpha^*(t,\Delta\omega)} = \frac{2\alpha(t,\Delta\omega)\beta(t,\Delta\omega)}{2|\alpha(t,\Delta\omega)|^2} = \frac{N_x(t,\Delta\omega) - \mathrm{i}N_y(t,\Delta\omega)}{N_z(t,\Delta\omega) - 1} \tag{2.13}$$

where the last equality follows quickly from (2.9) and (2.10*a*). Then $R(t,\Delta\omega)$ satisfies the Riccati equation

$$\frac{\mathrm{d}R(t,\Delta\omega)}{\mathrm{d}t} = \mathrm{i}\Delta\omega R(t,\Delta\omega) + r(t) + r^*(t)R^2(t,\Delta\omega). \tag{2.14}$$

Equation (2.14) is the same as the Riccati equation in [12].

If phase modulation is not allowed, then $\phi(t) = 0$ and the reflectivity function $r(t)$ is pure imaginary, so that $-r^*(t) = r(t)$. This reduces the asymmetric two-component wave system to a symmetric two-component wave system. For this special case, both [12] and (implicitly) [15] transform the Riccati equation (2.14) into a Schrödinger equation, using the standard transformation ((2.22) below) between the Riccati and Schrödinger equations. In [15] it is then demonstrated that in order for the solution of this Schrödinger equation to be asymptotically consistent with (2.5), the reflection coefficient of the entire wave system must be zero! This restricts the solutions to those associated with reflectionless potentials, as treated in [8–10].

Thus there seems to be a contradiction between the results of [15] and the results of [12] and this paper. The loophole is that the standard Riccati-to-Schrödinger equation transformation (2.22) does not preserve the scattering interpretation (this is what was really demonstrated in [15]). In a sense, the difficulty is that the standard transformation maps the Riccati equation to the *wrong* Schrödinger equation!

To see what is happening, let us examine the well known inverse scattering equations for a one-dimensional lossless constant-wavespeed acoustic medium. Such a medium is described by a symmetric two-component wave system; it has the same form as (2.12) when phase modulation is not allowed. The Riccati and Schrödinger scattering equations for this problem are familiar (e.g., see [16] for details), but we now show that the relation between them is *not* the standard mathematical transformation (2.22) between Riccati and Schrödinger equations. This explains the result of [15].

The basic equations for the medium are

$$\frac{\mathrm{d}p(z,\omega)}{\mathrm{d}z} = \rho(z)\omega^2 u(z,\omega) \qquad p(z,\omega) = -\rho(z)\frac{\mathrm{d}u(z,\omega)}{\mathrm{d}z} \tag{2.15}$$

where $p(z,\omega)$ is pressure, $u(z,\omega)$ is medium displacement, $\rho(z)$ is density, z is depth, and ω is frequency. Then

$$D(z,\omega) = p(z,\omega)/\sqrt{\rho(z)} + \mathrm{i}\omega\sqrt{\rho(z)}u(z,\omega) \tag{2.16a}$$

$$U(z,\omega) = p(z,\omega)/\sqrt{\rho(z)} - \mathrm{i}\omega\sqrt{\rho(z)}u(z,\omega) \tag{2.16b}$$

satisfy the symmetric two-component wave system (compare with (2.12) when $-r^*(t) = r(t)$; note the sign change between $\Delta\omega$ and ω)

$$\frac{\mathrm{d}}{\mathrm{d}z}\begin{pmatrix} D(z,\omega) \\ U(z,\omega) \end{pmatrix} = \begin{pmatrix} -\mathrm{i}\omega & r(z) \\ r(z) & \mathrm{i}\omega \end{pmatrix}\begin{pmatrix} D(z,\omega) \\ U(z,\omega) \end{pmatrix} \tag{2.17a}$$

$$r(z) = -\frac{1}{2\rho(z)}\frac{\mathrm{d}\rho(z)}{\mathrm{d}z} = -\frac{\mathrm{d}}{\mathrm{d}z}\log\sqrt{\rho(z)}. \tag{2.17b}$$

The Riccati equation associated with this system is (compare with (2.14))

$$\frac{\mathrm{d}R(z,\omega)}{\mathrm{d}z} = 2\mathrm{i}\omega R(z,\omega) + r(z) - r(z)R^2(z,\omega) \tag{2.18}$$

where we now define

$$R(z,\omega) = \frac{U(z,\omega)}{D(z,\omega)} = \frac{\mathrm{d}u(z,\omega)/\mathrm{d}z + \mathrm{i}\omega u(z,\omega)}{\mathrm{d}u(z,\omega)/\mathrm{d}z - \mathrm{i}\omega u(z,\omega)}. \tag{2.19}$$

The second equality follows from (2.15).

The Schrödinger scattering equation for a lossless acoustic medium is known to be (e.g. [16])

$$\left(\frac{d^2}{dz^2} + \omega^2 - V(z)\right) v(z,\omega) = 0 \tag{2.20a}$$

$$V(z) = \frac{1}{\sqrt{\rho(z)}} \frac{d^2}{dz^2} \sqrt{\rho(z)} \tag{2.20b}$$

$$v(z,\omega) = \sqrt{\rho(z)} u(z,\omega) = u(z,\omega) \exp\left(-\int_0^z r(z')dz'\right) \tag{2.20c}$$

where the second equality follows from (2.17*b*).

From (2.19) and (2.20*c*) it can be seen that the relation between the solutions $R(z,\omega)$ of the Riccati equation (2.18) and $v(z,\omega)$ of the Schrödinger scattering equation (2.20*a*) is

$$v(z,\omega) = \exp\left[\int_0^z -\left(i\omega \frac{1+R(z',\omega)}{1-R(z',\omega)} - r(z')\right) dz'\right]. \tag{2.21}$$

However, the standard transformation from the Riccati equation to the Schrödinger equation, as it was used in [15], is

$$v(z,\omega) = \exp\left[\int_{-\infty}^z \left(i\omega R(z',\omega) - r(z')\right) dz'\right] \tag{2.22}$$

Hence the standard transformation (2.22) does not give the usual Schrödinger scattering equation for a lossless medium.

Of course, the transformation (2.22) *does* lead to solutions of the Bloch transform inverse problem associated with reflectionless potentials, and this is quite useful [8–10]. However, it is now evident that our approach will lead to new classes of solutions. It should also be noted that [15] considers not (2.13) but

$$\frac{N_z(t,\Delta\omega) + iN_y(t,\Delta\omega)}{N_x(t,\Delta\omega) - 1}$$

and this leads to a Riccati equation different from (2.14).

3. Solution using the asymmetric Schur algorithm

In this section we briefly review the results of [13] on asymmetric two-component wave systems that pertain to the Zakharov–Shabat system (2.12). For more details and references, see [13].

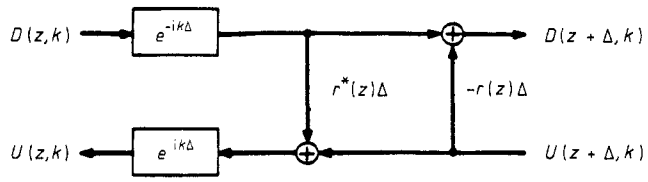

Figure 1. An infinitesimal section of the Zakharov–Shabat wave system (3.1).

3.1. The Zakharov–Shabat wave scattering system

The Zakharov–Shabat wave system

$$\frac{\mathrm{d}}{\mathrm{d}z}\begin{pmatrix} D(z,k) \\ U(z,k) \end{pmatrix} = \begin{pmatrix} -\mathrm{i}k & -r(z) \\ r^*(z) & \mathrm{i}k \end{pmatrix}\begin{pmatrix} D(z,k) \\ U(z,k) \end{pmatrix} \tag{3.1}$$

is a special case of the asymmetric two-component wave system treated in [13]. Here $D(z,k)$ and $U(z,k)$ are downgoing and upgoing waves, respectively, $r(z)$ is the reflectivity function, z is depth (increasing downward), and k may be either frequency or wavenumber. The system (3.1) describes the scattering medium illustrated in figure 1. This medium varies smoothly for $0 < z < L$, and it is homogeneous (i.e. $r(z) = 0$) for $z < 0$ and $z > L$.

In the time domain (3.1) becomes the pair of equations

$$\left(\frac{\partial}{\partial z} + \frac{\partial}{\partial t}\right)\check{D}(z,t) = -r(z)\check{U}(z,t) \tag{3.2a}$$

$$\left(\frac{\partial}{\partial z} - \frac{\partial}{\partial t}\right)\check{U}(z,t) = r^*(z)\check{D}(z,t) \tag{3.2b}$$

where $\check{D}(z,t) = \int_{-\infty}^{\infty} D(z,k)\exp(\mathrm{i}2\pi kt)\mathrm{d}k$ is the inverse Fourier transform of $D(z,k)$, and similarly for $\check{U}(z,t)$. $D(z,k)$ and $U(z,k)$ are considered to be waves since (3.2) describes quantities that propagate in increasing and decreasing depth z as t increases. The reflectivity function $r(z)$ describes how much of each wave is reflected into the other wave at each z. If $r(z) = 0$ then the medium is locally homogeneous, and no scattering occurs.

3.2. Inverse scattering problem

Now let the solution to (3.1) have the following asymptotic forms:

$$D(z,k) = \mathrm{e}^{-\mathrm{i}kz} \qquad U(z,k) = R(k)\mathrm{e}^{\mathrm{i}kz} \qquad z \le 0 \tag{3.3a}$$

$$D(z,k) = T(k)\mathrm{e}^{-\mathrm{i}kz} \qquad U(z,k) = 0 \qquad z > L. \tag{3.3b}$$

This is the same as letting the solution to (3.2) have the following asymptotic forms:

$$\check{D}(z,t) = \delta(t-z) \qquad \check{U}(z,t) = \check{R}(t+z) \qquad z \le 0 \tag{3.4a}$$

$$\check{D}(z,t) = \check{T}(t-z) \qquad \check{U}(z,t) = 0 \qquad z > L. \tag{3.4b}$$

These equations describe an inverse scattering experiment that consists of probing the medium with an impulsive plane wave $\delta(t-z)$, incident from above and propagating

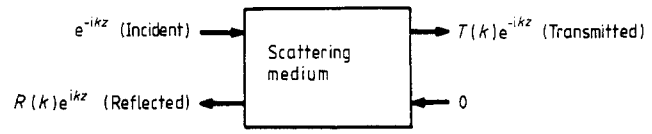

Figure 2. An inverse scattering experiment with probing from the left resulting in reflection response $R(k)$ and transmission response $T(k)$.

downward, and getting back a reflection response $\check{R}(t)$ that is causal and a transmission response $\check{T}(t)$ at the far end of the medium. This is illustrated in figure 2.

Since $\check{R}(t)$ is causal, it is clear that $\check{D}(z,t)$ and $\check{U}(z,t)$ have the forms

$$\check{D}(z,t) = \delta(t-z) + \tilde{D}(z,t)1(t-z) \tag{3.5a}$$

$$\check{U}(z,t) = \tilde{U}(z,t)1(t-z) \tag{3.5b}$$

where $\tilde{D}(z,t)$ and $\tilde{U}(z,t)$ are the smooth parts of $\check{D}(z,t)$ and $\check{U}(z,t)$ (both of which jump at $t=z$), and where $1(\,)$ is the unit step or Heaviside function. Equations (3.5) are simply a statement of causality.

Inserting (3.5) into (3.2) and using a propagation of singularities argument (this amounts to equating coefficients of $\delta(t-z)$) yields

$$\left(\frac{\partial}{\partial z} + \frac{\partial}{\partial t}\right)\tilde{D}(z,t) = -r(z)\tilde{U}(z,t) \tag{3.6a}$$

$$\left(\frac{\partial}{\partial z} - \frac{\partial}{\partial t}\right)\tilde{U}(z,t) = r^*(z)\tilde{D}(z,t) \tag{3.6b}$$

$$r^*(z) = -2\tilde{U}(z,z^+) = -2\lim_{t\downarrow z}\tilde{U}(z,t). \tag{3.6c}$$

The derivation of (3.6) from (3.2) is analogous to the derivation of transport equations for a system of partial differential equations.

3.3. The asymmetric Schur algorithm

Discretising depth z and time t into integer multiples of a small constant Δ and using forward differences, (3.6) discretises into

$$\begin{pmatrix}\tilde{D}(z+\Delta,t+\Delta)\\ \tilde{U}(z+\Delta,t-\Delta)\end{pmatrix} = \begin{pmatrix}1 & -r(z)\Delta\\ r^*(z)\Delta & 1\end{pmatrix}\begin{pmatrix}\tilde{D}(z,t)\\ \tilde{U}(z,t)\end{pmatrix} \tag{3.7a}$$

$$r^*(z)\Delta = -\tilde{U}(z,z)/\tilde{D}(z,z) \tag{3.7b}$$

$$D(0,t) = 0 \qquad U(0,t) = \check{R}(t). \tag{3.7c}$$

Equations (3.7) constitute a layer-recursive procedure for reconstructing $r(z)$ from $\check{R}(t)$. Note the transmission response $\check{T}(t)$ is not needed.

3.4. Comments

(I) Equations (3.7) differ from the well known Schur algorithm only in that the reflectivity functions $r(z)$ and $-r^*(z)$ are unequal. This is why a straightforward discretisation is used—to identify this inverse scattering problem solution with a well known numerically stable algorithm. Indeed, by inserting an additional factor of $1/\sqrt{1+|r(z)\Delta|^2}$ the transformation at each step becomes a multiplication by a unitary matrix (note this additional factor cancels out in (3.7*b*)).

(II) In physical inverse scattering problems, wave systems like (3.1) describe *absorbing* media [13]. For example: (i) acoustic media with constant density and wave speed, but varying absorption (Maxwell model); (ii) electromagnetic media with constant permittivity and permeability, but varying conductivity.

(III) In fact, (3.7) is a special case of the asymmetric Schur algorithm. Even though the reflectivity functions are unequal, we can obviously compute one from the other. Hence reflection data from one end only of the scattering medium are sufficient to reconstruct it, even though the medium is lossy.

(IV) These types of absorbing media can also be formulated as Schrödinger equation inverse potential problems [14]. The potential turns out to be complex, with an imaginary part linearly proportional to wavenumber k. Again the reflection coefficient $R(k)$ constitutes sufficient data; however, solution of an integral equation replaces (3.7) [14].

(V) The Born approximation is commonly used in inverse scattering problems. This is a single-scattering assumption in which only direct or primary scattering events are considered; multiple scattering is neglected. Here this amounts to neglecting the coupling in (3.7*a*), which simplifies to

$$-r^*(z) = \tilde{U}(z,z) = \tilde{U}(0,2z) = \check{R}(2z) \tag{3.8}$$

i.e. each value of $\check{R}(t)$ is assumed to come directly from a reflection of the impulse $\delta(t-z)$ from $-r^*(z)$. This will be used to interpret linearisation of the Bloch transform in subsection 4.4.

(VI) Equation (3.7*b*) follows immediately from (3.7*a*) by setting $t = z$ and noting that $\tilde{U}(z+\Delta, z-\Delta)$ is zero by causality. Note that a factor of 2 in (3.6*c*) disappears in the discretisation.

4. Solution of the inverse Bloch transform problem

Comparing (2.12) and (3.1), we see that $\alpha^*(t,\Delta\omega)$ and $\beta(t,\Delta\omega)$ correspond to $D(z,k)$ and $U(z,k)$, respectively, and that t and $\Delta\omega/2$ in (2.12) correspond to z and k in (3.1). It is clear that the asymmetric Schur algorithm can be used to compute $r(t)$ in (2.12), provided that a scattering interpretation can be attached to (2.12) and a reflection response characterising the desired final magnetisation state can be produced.

4.1. Scattering interpretation

The initial magnetisation state is given by (2.8). Inserting (2.8) into (2.9) and (2.10), and repeating (2.10*c*), gives

$$N_z(t,\Delta\omega) = |\beta(t,\Delta\omega)|^2 - |\alpha(t,\Delta\omega)|^2 \tag{4.1a}$$

$$N_x(t,\Delta\omega) - \mathrm{i}N_y(t,\Delta\omega) = -2\alpha(t,\Delta\omega)\beta(t,\Delta\omega) \tag{4.1b}$$

$$|\alpha(t,\Delta\omega)|^2 + |\beta(t,\Delta\omega)|^2 = 1. \tag{4.1c}$$

Equations (4.1) describe the time evolution of $N(t, \Delta\omega)$ directly in terms of the quantities $\alpha(t, \Delta\omega)$ and $\beta(t, \Delta\omega)$ in (2.12), for the initial magnetisation state (2.8).

For $t = 0$ and $N(t, \Delta\omega)$ as in (2.8), the solution to (4.1) is

$$\alpha(0, \Delta\omega) = 1 \qquad \beta(0, \Delta\omega) = 0. \tag{4.2}$$

This is illustrated in figure 3, from which we see that $\alpha^*(t, \Delta\omega)$ and $\beta(t, \Delta\omega)$ are the Jost solutions for a scattering experiment with an impulse incident from the *right*. Thus, although we have successfully attached a scattering interpretation to (2.12), we also seem to require the (unknown) Jost solutions at $t = T$. We now show that this is not so.

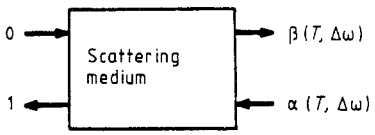

Figure 3. The inverse scattering experiment associated with the Bloch transform. $\alpha(T\Delta\omega)$ and $\beta(T\Delta\omega)$ are as defined in (2.12).

4.2. Initialisation at t=T

Let the medium represented by (2.12) be probed from the *right* with an impulse, resulting in a reflection response $R(T, \Delta\omega)$ and a transmission response $T(T, \Delta\omega)$ (this is as in figure 2, but with left and right interchanged). By linearity, we can divide the responses in figure 3 by $\alpha^*(t, \Delta\omega)$. Comparing the result with figure 2 (with left and right interchanged), we have

$$R(T, \Delta\omega) = \frac{\beta(T, \Delta\omega)}{\alpha^*(T, \Delta\omega)} = \frac{|\beta(T, \Delta\omega)|}{|\alpha(T, \Delta\omega)|} \exp\left(\arg[\alpha(T, \Delta\omega)] + \arg[\beta(T, \Delta\omega)]\right)$$

$$T(T, \Delta\omega) = \frac{1}{\alpha^*(T, \Delta\omega)}. \tag{4.3}$$

This shows that it is *not* necessary to find the Jost solutions at $t = T$; merely specifying $R(T, \Delta\omega)$, rather than $\alpha^*(T, \Delta\omega)$ and $\beta(T, \Delta\omega)$ separately, is sufficient to compute the $r(t)$.

Note that we have assumed $\alpha^*(t, \Delta\omega)$ has no zeros in the lower half of the complex $\Delta\omega$ plane; this is tantamount to assuming there are no bound states. In practice, we will *choose* reflection responses without bound states, to give results different from [7–10].

4.3. Summary of procedure

Given a desired final magnetisation state $N(T, \Delta\omega)$, the Schur algorithm is initialised at $t = T$ as follows.

(i) Solve (4.1) for $|\alpha(T, \Delta\omega)|$, $|\beta(T, \Delta\omega)|$, and $\arg[\alpha(T, \Delta\omega)] + \arg[\beta(T, \Delta\omega)]$.

(ii) Compute $R(T, \Delta\omega)$ using (4.3). Note that the three quantities computed above *uniquely* specify $R(T, \Delta\omega)$.

(iii) Compute

$$\check{R}(\tau) = \mathscr{F}^{-1}_{\Delta\omega/2 \to \tau}\{R(T, \Delta\omega)\} \tag{4.4}$$

where $R(T,\Delta\omega)$ is analytically extended into the complex $\Delta\omega$ plane so that $\check{R}(\tau)$ is causal. Mathematically, this is similar to an inverse Laplace transform; in practice, it is easy to choose $R(T,\Delta\omega)$ so that this can be avoided (see section 5).

(iv) Initialise the Schur algorithm using $\check{R}(\tau)$.

(v) Run the Schur algorithm, computing $r(t)$. Reverse them in time (replace $r(t)$ with $r(T-t)$).

(vi) Compute the amplitude modulation $B_1(t)$ and phase modulation $\phi(t)$ achieving the desired $N(T,\Delta\omega)$ using (2.12*b*).

The only difficulty is that arbitrary selection of $\alpha(T,\Delta\omega)$ and $\beta(T,\Delta\omega)$ can lead to $r(t)$ (and therefore modulations) that are impractically large, or of too long a duration. Hence some judgment must be exercised in selecting the exact shape of the final $M(T,\Delta\omega)$ so that the $r(t)$ leading to it constitute a practical modulation. The Born approximation (see below) will often give a rough idea of the resulting $r(t)$.

Note that this procedure allows trade-offs to be identified quickly.

(i) If the selective excitation region is too narrow, the $r(t)$ will have long duration (infinitely long for the case of an infinitely narrow slice).

(ii) The larger the angle of flip, the larger $r(t)$, hence the amplitude modulation $B_1(t)$, will be.

4.4. The Born approximation to the Bloch transform

Applying the Born approximation (see section 3) to this procedure is most illuminating. Applying (3.8) directly, and using (4.1) and (4.3), gives

$$(\mathrm{i}/2)\gamma B_1(T-t)\mathrm{e}^{-\mathrm{i}\phi(T-t)} = -r^*(T-t) = \mathscr{F}^{-1}(R(T,\Delta\omega)) = \mathscr{F}^{-1}\left(\frac{\beta(T,\Delta\omega)}{\alpha^*(T,\Delta\omega)}\right)$$

$$= \mathscr{F}^{-1}\left(\frac{2\alpha(T,\Delta\omega)\beta(T,\Delta\omega)}{2|\alpha(T,\Delta\omega)|^2}\right) = \mathscr{F}^{-1}\left(\frac{N_x(T,\Delta\omega)-\mathrm{i}N_y(T,\Delta\omega)}{N_z(T,\Delta\omega)+1}\right). \tag{4.5}$$

This shows that the inverse Bloch transform can be approximated by an inverse Fourier transform. This is the same result obtained in [2, 3] by linearising a series expansion. Note that the factor of 2 in (3.8) is cancelled when $\mathrm{i}\Delta\omega/2$ replaces $\mathrm{i}k$ in the Fourier transform; the two-way traveltime is replaced with one-way traveltime due to the time scaling.

Note that the Born approximation interpretation lends physical insight; examination of the $r(t)$ obtained using the Born approximation can be used to decide whether multiple reflections in (2.12) will be significant enough to warrant using the Schur algorithm instead of the Born approximation.

Note also that in the Born approximation the $r(t)$ are directly proportional to the amplitude modulation $B_1(t)$. Note also that the larger $N_x(T,\Delta\omega)-\mathrm{i}N_y(T,\Delta\omega)$ is, the bigger the $r(t)$ will be. Hence for large pulse amplitudes, or large tip angles, the Schur algorithm should be used.

5. Numerical examples

Some numerical examples of the procedure are given. These are intended to illustrate how the procedure works: a suitable $R(T,\Delta\omega)$ is chosen, and the procedure outputs $r(t)$, which is related to the modulation by (2.12*b*). The modulation is then inserted into

the modified Bloch equation (2.5) to determine the resulting final magnetisation state. The two problems considered are 90° and 180° rotations of proton spins in a thin slice.

In using this procedure, it is of course necessary to scale the variables appropriately. To see how this is done, consider the following example. Suppose we are interested in flipping proton spins in the middle of a sample 20 cm long. The maximum resonance offset computed from (2.6) is then (4260 Hz G^{-1})(1 G cm^{-1})(10 cm) = 42.6 kHz. Now define the scaled variables

$$\Delta\omega' = \Delta\omega/(85.2 \text{ kHz}) \qquad r'(t) = r(t)/(85.2 \text{ kHz}) \qquad t' = t(85.2 \text{ kHz}). \tag{5.1}$$

The primed variables also satisfy (2.12), but the range of $\Delta\omega$ has been scaled to the interval $[-\frac{1}{2}, \frac{1}{2}]$. This allows use of the discrete Fourier transform; the integer time values are multiples of 1/(85.2 kHz)=11.7 μs. The computed values $r'(t)$ must be scaled using (5.1) to obtain the final results. Since primed variables are used in all the computations, we omit the primes in the following for convenience.

In the results shown here, a 128-point discrete Fourier transform is used. Both $r(t)$ and the resulting $N_z(T, \Delta\omega)$ are displayed with their arguments ranging from 1 through 128; the actual range for $N_z(T, \Delta\omega)$ is -0.5 through 0.5. Computation time on a PC-AT with co-processor was 15 minutes for each run.

5.1. 90° rotation: initialisation

The goal here is to achieve a final magnetisation state

$$N(T, \Delta\omega) = \begin{cases} [0, 0, -1]^{\mathrm{T}} & \text{for most } \Delta\omega \\ [1, 0, 0]^{\mathrm{T}} & \text{for } \Delta\omega \approx \Delta\omega_o \end{cases} \tag{5.2}$$

where $\Delta\omega_o$ is the slice selected. This corresponds to a 90° rotation from the z direction to the x direction. Inserting (5.2) into (4.1) results in

$$\begin{aligned} &|\alpha(T, \Delta\omega)| = 1 \qquad |\beta(T, \Delta\omega)| = 0 \qquad \text{for most } \Delta\omega \\ &|\alpha(T, \Delta\omega)| = |\beta(T, \Delta\omega)| = 0.7071 \qquad \text{for } \Delta\omega \approx \Delta\omega_o \\ &\arg[\alpha(T, \Delta\omega)] + \arg[\beta(T, \Delta\omega)] = 0. \end{aligned} \tag{5.3}$$

This leads to a reflection response

$$R(T, \Delta\omega) = \begin{cases} 0 & \text{for most } \Delta\omega \\ 1 & \text{for } \Delta\omega \approx \Delta\omega_o. \end{cases} \tag{5.4}$$

$r(t)$ will depend on the exact shape of $R(T, \Delta\omega)$ near $\Delta\omega_o$.

5.2. 90° rotation: numerical results

An obvious choice for $R(T, \Delta\omega)$ is

$$R(T, \Delta\omega) = \begin{cases} 1 & \text{for } |\Delta\omega| < 0.025 \\ 0 & \text{elsewhere} \end{cases} \tag{5.5}$$

which should result in a 90° flip in a thin slice in the middle. The x component $N_x(T, \Delta\omega)$ of the final magnetisation state resulting from integration of the modified Bloch equation (2.5) is shown in figure 4(*a*). The resulting $r(t)$ outputted by the Schur

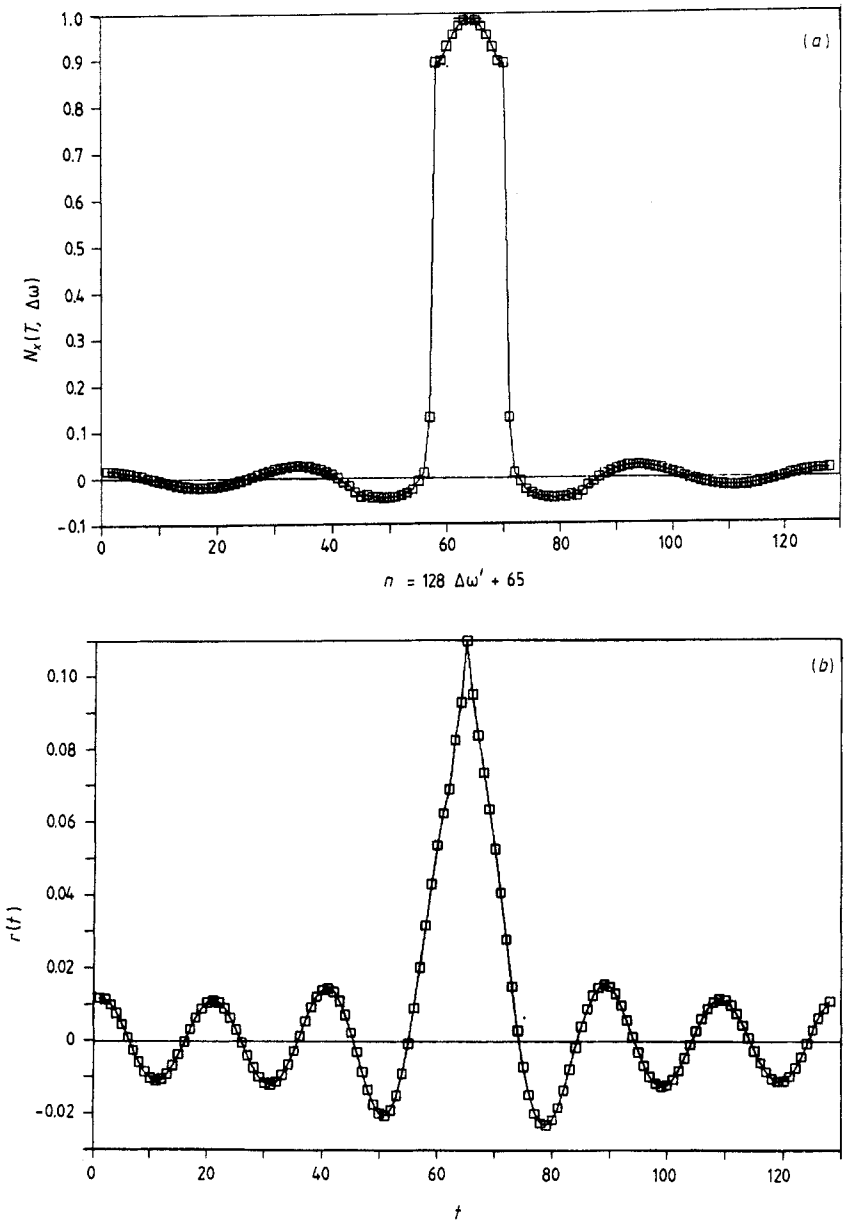

Figure 4. (*a*) The x component of the final magnetisation state $N(T\Delta\omega)$ plotted against slice number ($n = 128\Delta\omega' + 65$) for (5.5). The spins are flipped 90° in the region in the middle. (*b*) The reflectivity function $r(t)$ outputted by the Schur algorithm with input (5.5). $r(t)$ represents the amplitude modulation that achieves the $N_x(T\Delta\omega)$ shown in figure 4(*a*).

algorithm is shown in figure 4(*b*). It is evident that $r(t)$ has successfully flipped the proton spins by 90° in the slice shown. Although we do not show it here, the time evolution of $N(t, \Delta\omega)$ is a gradual reduction in the z component in the middle, and a corresponding growth in the x component.

Note that $r(t)$ is very close to a sinc function, which is the shifted inverse Fourier transform of (5.5). This is the result of applying the Born approximation (4.5) to (5.5). For a 90° flip, the Born approximation works quite well. It should be noted that the use of a sinc function to achieve a 90° flip is quite common [3].

It is also possible to achieve selective excitation of slices not at the origin. Suppose it is desired to flip spins 90° in a different slice. Figure 5 gives the $r(t)$ and resulting $N_x(T,\Delta\omega)$ for a shifted version of (5.5). The selected slice is now off-centre, but otherwise has characteristics similar to those of figure 4(*a*). $r(t)$ is now complex; phase modulation is necessary to achieve selective excitation of off-centre slices. An alternative is to physically move the object being imaged; use of phase modulation sometimes may be more convenient.

To see why $r(t)$ has the form shown in figure 5(*b*), note that shifting $R(T,\Delta\omega)$ by an amount Ω corresponds to multiplication of $\mathscr{F}^{-1}\{R(T,\Delta\omega)\}$ by $e^{i\tau\Omega} = \cos\tau\Omega + i\sin\tau\Omega$. Thus, in the Born approximation, $r(t)$ will itself be modulated by this complex function. This is what is happening in figure 5(*b*).

5.3. 180° rotation: initialisation

The goal is now to achieve a final magnetisation state

$$N(T,\Delta\omega) = \begin{cases} [0,0,-1]^T & \text{for most } \Delta\omega \\ [0,0,1]^T & \text{for } \Delta\omega \approx \Delta\omega_o \end{cases} \tag{5.6}$$

where $\Delta\omega_o$ is the slice selected. This corresponds to a 180° rotation from the z direction to the x direction. Inserting (5.6) into (4.1) results in

$$\begin{aligned} &|\alpha(T,\Delta\omega)| = 1 \qquad |\beta(T,\Delta\omega)| = 0 \qquad \text{for most } \Delta\omega \\ &|\alpha(T,\Delta\omega)| = 0 \qquad |\beta(T,\Delta\omega)| = 1 \qquad \text{for } \Delta\omega \approx \Delta\omega_o \\ &\arg[\alpha(T,\Delta\omega)] + \arg[\beta(T,\Delta\omega)] = \text{irrelevant.} \end{aligned} \tag{5.7}$$

This leads to a reflection response

$$R(T,\Delta\omega) = \begin{cases} 0 & \text{for most } \Delta\omega \\ \infty & \text{for} \Delta\omega \approx \Delta\omega_o. \end{cases} \tag{5.8}$$

Obviously it will be necessary to approximate (5.8) in some way. A large amplitude can be expected to result in flip angles slightly less than 180°.

5.4. 180° rotation: numerical results

A first choice for $R(T,\Delta\omega)$ is

$$R(T,\Delta\omega) = \begin{cases} 10 & \text{for } |\Delta\omega| < 0.025 \\ 0 & \text{elsewhere} \end{cases} \tag{5.9}$$

which should result in a large flip (probably less than 180°) in a thin slice in the middle. The resulting $r(t)$ and $N_z(T,\Delta\omega)$ are shown in figure 6. Note that the excitation is quite selective, but the flip angle is only about 135°. However, $r(t)$ looks nothing like a sinc function, so that the Born approximation is not working at all. Since the $R(T,\Delta\omega)$ and $r(t)$ are much bigger than before, this is not surprising.

Increasing the amplitude of $R(T,\Delta\omega)$ resulted in even spikier $r(t)$ functions, and the form of $N_z(T,\Delta\omega)$ only got worse: the flip angle in the selected slice increased toward

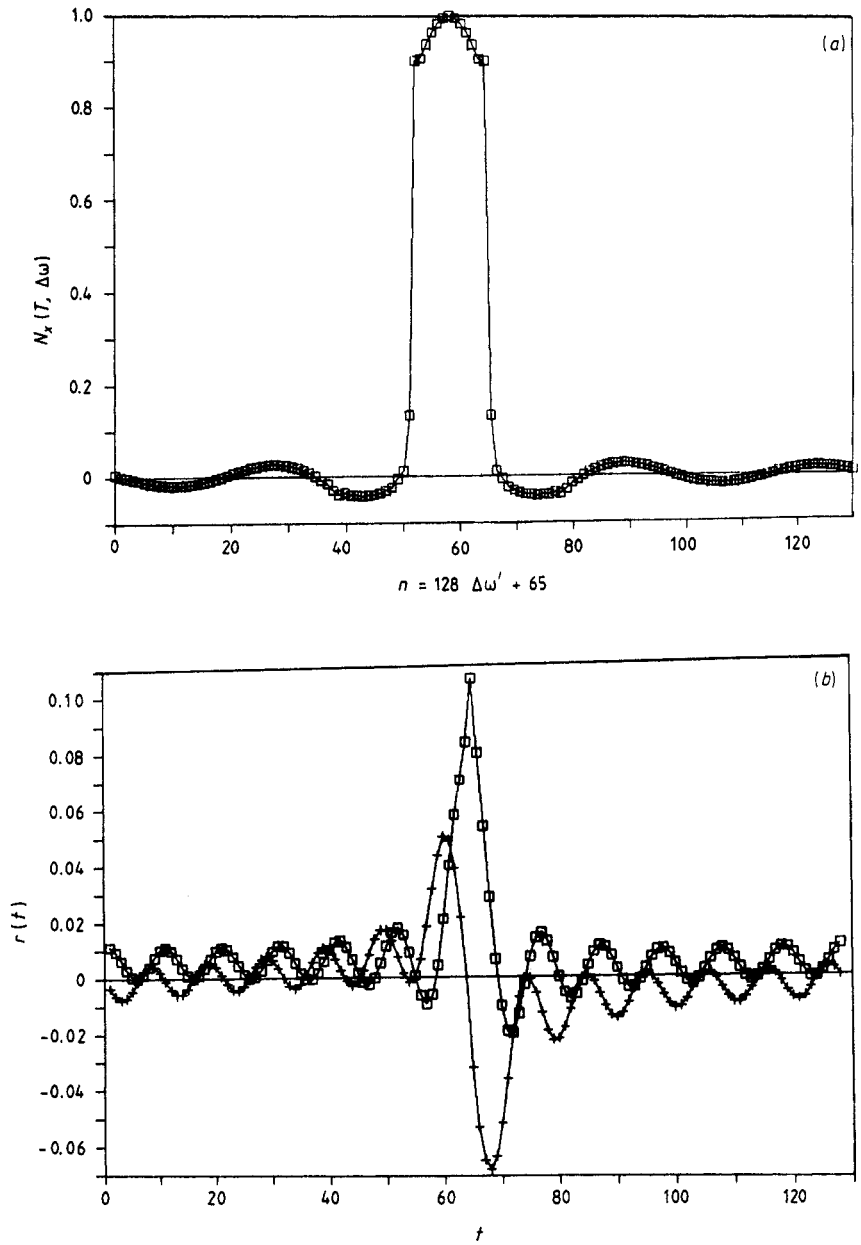

Figure 5. The x component of the final magnetisation state $N(T\Delta\omega)$ plotted against slice number ($n = 128\Delta\omega' + 65$) for a shifted version of (5.5). The spins are flipped 90° in the slice which is no longer in the middle. (*b*) The real and imaginary parts of the reflectivity function $r(t)$ outputted by the Schur algorithm with input a shifted version of (5.5). $r(t)$ represents the amplitude and phase modulation (see (2.12*b*)) that achieves the $N_x(T\Delta\omega)$ shown in figure 5(*a*).

180° very slowly with increasing amplitude of $R(T, \Delta\omega)$, while the region outside the slice began to be excited.

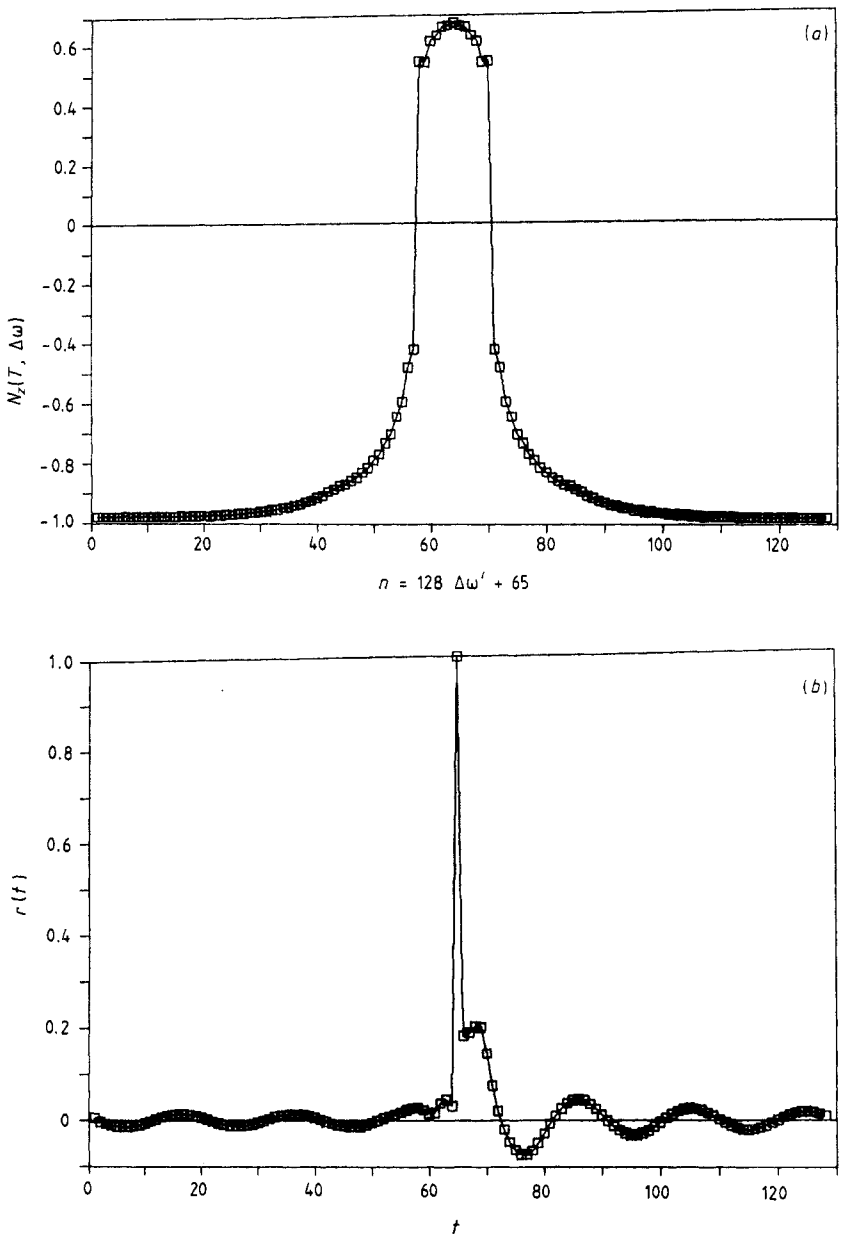

Figure 6. (*a*) The z component of the final magnetisation state $N(T\Delta\omega)$ plotted against slice number ($n = 128\Delta\omega' + 65$) for (5.9). The spins are flipped about 135° in the region in the middle. (*b*) The reflectivity function $r(t)$ outputted by the Schur algorithm with input (5.9). $r(t)$ represents the amplitude modulation that achieves the $N_z(T\Delta\omega)$ shown in figure 6(*a*).

Another modulation signal commonly used is a Gaussian signal [1], resulting (in the Born approximation) in a Gaussian slice profile. This suggests trying

$$R(T, \Delta\omega = k/128) = 7.1(0.995)^{k^2} \qquad -64 \leq k < 64 \tag{5.10}$$

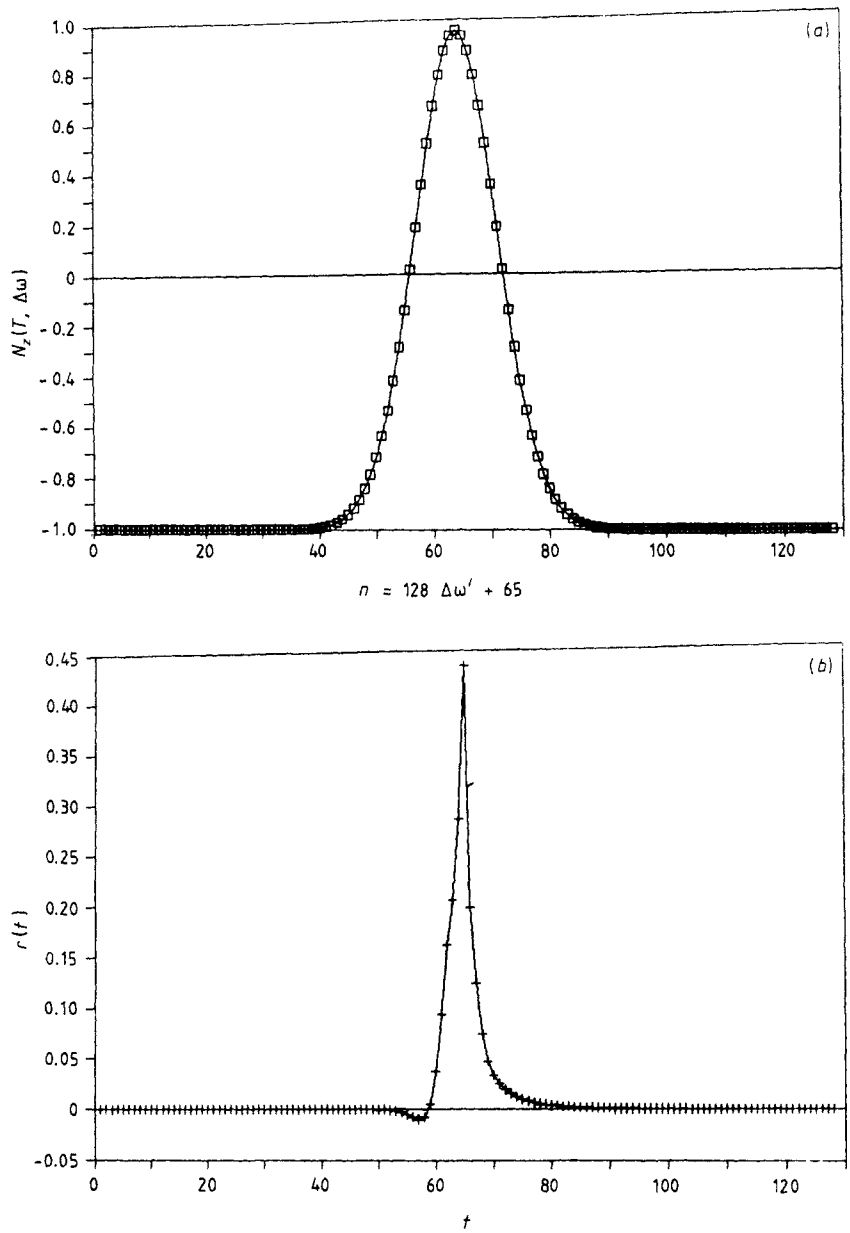

Figure 7. The z component of the final magnetisation state $N(T\Delta\omega)$ plotted against slice number ($n = 128\Delta\omega' + 65$) for (5.10). The spins are flipped 180° in the middle. (*b*) The reflectivity function $r(t)$ outputted by the Schur algorithm with input (5.10). $r(t)$ represents the amplitude modulation that achieves the $N_z(T\Delta\omega)$ shown in figure 7(*a*).

which should result in a large flip angle in the centre of a Gaussian-shaped slice. The resulting $r(t)$ and $N_z(T, \Delta\omega)$ are shown in figure 7. Note that the Gaussian slice is realised quite nicely, while the $r(t)$, although not a Gaussian pulse, looks more like a Gaussian pulse than figure 6(*a*) looks like a sinc pulse. This suggests that the Born approximation breaks down more slowly for Gaussian-shaped pulses.

The results shown in this section seem to be comparable to those obtained using reflectionless potentials in [8–10], although the modulation functions are quite different. In particular, the results of this paper are easier to compare with known results using Gaussian and sinc pulses. The most important point is that a different family of modulation functions can now be obtained; this complements the results of [8–10].

6. Conclusion

A new procedure has been proposed for inverting the Bloch transform in magnetic resonance imaging. Following [12], the Bloch transform is recast as a Zakharov–Shabat two-component wave system, in which the reflectivity function $r(t)$ is related to the modulation needed to achieve a desired final magnetisation state $M(T, \Delta\omega)$. This is a special case of the inverse scattering problem for asymmetric two-component wave systems treated in [13]. Hence the asymmetric Schur algorithm from [13] can be applied to this problem. Due to the special form of the Zakharov–Shabat system, reflection data from only one side are sufficient to reconstruct $r(t)$, even though the scattering medium represented by the system (*not* the medium be magnetic resonance imaged) is lossy.

There are considerable grounds for further work. The problem of selecting an exact form of $R(T, \Delta\omega)$ that will lead to a 'reasonable' $r(t)$ is still not pinned down, although the Born approximation helps—we need Fourier transform pairs that are narrow in both time and frequency. A more interesting problem is considering initial magnetisation states $M(x, y, z, 0)$ different from $[0, 0, -1]^T$. What set of initial states can be treated, and what set of final states can be attained from it? The method proposed here will work on any $M(x, y, z, 0)$ invariant in x and y (all we need is $\alpha(0, \Delta\omega) = 1$ and $\beta(0, \Delta\omega) = 0$), but it is not clear what final states correspond to realisable reflection responses.

Acknowledgments

It is a pleasure to acknowledge the hospitality of the Institute for Mathematics and its Applications at the University of Minnesota, where the author learned about this problem. Several conversations with Andy Hasenfeld and Alberto Grunbaum formulated the problem. Der-Shan Luo performed the computer simulations. This work was supported in part by the Institute for Mathematics and its Applications, and in part by the National Science Foundation under grant #MIP-8858082.

References

[1] Hinshaw W and Lent A 1983 An introduction to NMR imaging from the Bloch equation to the imaging equation *Proc. IEEE* **71** 338

[2] Grunbaum F A 1985 An inverse problem related to the Bloch equations and a non-linear Fourier transform *Inverse Problems* **1** L25

[3] Hoult D 1979 The solution of the Bloch equations in the presence of a varying B_1 field *J. Magn. Res.* **35** 69

[4] Baum J, Tycko R and Pines A 1983 *J. Chem. Phys.* **79** 4643

[5] Connolly S, Nishimura D and Macovski A 1986 *IEEE Trans. Med. Imag.* **MI-5** 106

[6] Murdoch J, Lent A and Kritzer M 1987 Computer-optimised narrowband pulses for multislice imaging *J. Magn. Res.* **74** 226
[7] Grunbaum F A and Hasenfeld A 1986 An exploration of the invertibility of the Bloch transform *Inverse Problems* **2** 75
[8] Grunbaum F A and Hasenfeld A 1988 An exploration of the invertibility of the Bloch transform II *Inverse Problems* **4** 485
[9] Hasenfeld A 1987 A connection between the Bloch equations and the Korteweg–de Vries equation *J. Magn. Res.* **72** 509.
[10] Hasenfeld A 1987 The Bloch equations and the Korteweg-de Vries hierarchy *Inverse Problems* **3** L45
[11] Ablowitz M and Segur H 1984 *Solitons and the Inverse Scattering Transform* (Philadelphia, PA: SIAM)
[12] Grunbaum F A 1988 Soliton mathematics in signal processing *Preprint* Department of Mathematics, University of California, Berkeley, CA
[13] Yagle A E 1989 One-dimensional inverse scattering problems: an asymmetric two-component wave system framework *Inverse Problems* **5** 641
[14] Jaulent M 1976 Inverse scattering problems in absorbing media *J. Math. Phys.* **17** 1351
[15] Hasenfeld A 1987 Scattering is not the way to invert the Bloch transform *Inverse Problems* **3** L9
[16] Newton R G 1981 Inversion of reflection data for layered media: a review of exact methods *Geophys. J. R. Astron. Soc.* **65** 191